

Probing Fermi surface parity with spin resolved transverse magnetic focussing

M. J. Rendell,^{1,*} S. D. Liles,¹ S. Bladwell,¹ A. Srinivasan,¹ O. Klochan,²
I. Farrer,³ D. A. Ritchie,⁴ O. P. Sushkov,¹ and A. R. Hamilton¹

¹*School of Physics, University of New South Wales, Sydney, NSW 2052, Australia*

²*University of New South Wales Canberra, Canberra, ACT 2600, Australia*

³*Department of Electronic and Electrical Engineering, University of Sheffield, Sheffield, S1 3JD, UK*

⁴*Cavendish Laboratory, University of Cambridge, Cambridge, CB3 0HE, UK*

(Dated: March 11, 2024)

Measurements of the Fermi surface are a fundamental technique for determining the electrical and magnetic properties of solids. In 2D systems, the area and diameter of the Fermi surface is typically measured using Shubnikov-de Haas oscillations and commensurability oscillations respectively. However, these techniques are unable to detect changes in the parity of the Fermi surface (i.e. when $+k \neq -k$). Here, we show that transverse magnetic focussing can be used to detect such changes, because focussing only measures a well defined section of the Fermi surface and does not average over $+k$ and $-k$. Furthermore, our results show that focussing is an order of magnitude more sensitive to changes in the Fermi surface than other 2D techniques, and could be used to investigate similar Fermi surface changes in other 2D systems.

Techniques for measuring the Fermi surface have existed since the early 1930s [1, 2], and are a powerful way to probe electronic and magnetic properties of metals, semiconductors, superconductors and heavy fermion compounds [3–6]. In 2D systems, the area of the Fermi surface is typically measured using Shubnikov-de Haas oscillations, while the diameter can be measured using commensurability oscillations. [7–12]. These techniques allow for the size and asymmetry of the Fermi surface to be found experimentally, however they are not able to resolve a change in the parity of the Fermi surface (i.e. when $E(+k) \neq E(-k)$) as this would be averaged out over the whole Fermi surface.

A lesser used technique is transverse magnetic focussing, which was originally proposed as a technique for probing the Fermi surface of metals [13–15]. Transverse magnetic focussing is unique among methods for measuring 2D Fermi surfaces in that it uses point contacts for injection and detection of charge. This means that focussing is able to measure a well defined section of the Fermi surface, as the charge carriers do not complete a full orbit [16–22]. As a result, focussing is able to detect changes in the parity of the Fermi surface. These changes are not visible in other techniques as they are averaged out over the full Fermi surface. In addition, the use of point contacts makes focussing extremely sensitive, allowing it to probe spin and charge dynamics including branched electron flow, small-angle scattering, spin separation and spin precession [23–28].

Here, we show that focussing can be used to detect a change in the parity of the Fermi surface of 2D holes in a GaAs quantum well created by an in-plane magnetic field (B_{\parallel}). This change in parity arises from an interplay between B_{\parallel} and the Rashba spin-orbit interaction of holes in GaAs/AlGaAs. Additionally, we find that focussing is at least an order of magnitude more sensitive to changes in the Fermi surface than previous measurements using

commensurability oscillations [12]. While the exact effect we observe here is specific to holes in GaAs, this technique could be used to investigate similar changes to the parity of the Fermi surface in other 2D systems.

The magnetic focussing sample is fabricated on a GaAs/Al_{0.33}Ga_{0.67}As heterostructure with a 15nm GaAs quantum well confining the 2D hole gas (2DHG) 85nm below the surface. The 2DHG is induced in accumulation mode (no doping) by applying a negative voltage to an overall top gate. The use of an undoped heterostructure avoids device instability in the gate defined nanostructures which create the focussing geometry [29, 30]. Figure 1 shows an SEM of the sample with lithographic split gates used to define the focussing geometry. The overlay indicates the electrical measurement setup and the orientation of the in-plane magnetic field. To perform focussing, a constant current of holes ($I_{SD} = 5\text{nA}$) is injected through a quantum point contact (QPC), and the resulting focussing signal is measured as a voltage across a second QPC. This is performed as a four terminal measurement with a pair of lock-in amplifiers at low frequency (17 Hz). When the perpendicular magnetic field (B_{Focus}) is such that the focussing diameter (d_{Focus}) is equal to the spacing between QPCs, a peak is observed in the focussing voltage. These peaks occur when the magnetic field is an integer multiple of [16]

$$B_{\text{Focus}} = \frac{2\hbar k_F}{ed_{\text{Focus}}}$$

Where k_F is the Fermi momentum. All measurements in this work use a focussing diameter $d_{\text{Focus}} = 800\text{nm}$ at a 2D density of $n_{2D} = 1.89 \times 10^{11} \text{ cm}^{-2}$, ($V_{\text{TG}} = -1.35\text{V}$) with a mobility of $760\,000 \text{ cm}^{-2} \text{ V s}$ and mean free path of $5.3\mu\text{m}$. The QPCs have lithographic dimensions of $300 \times 300 \text{ nm}$ and are biased to $G=2e^2/h$ to inject and detect both spin polarisations. The sample is measured in a He dilution system with a $9/5/1 \text{ T}$ vector magnet

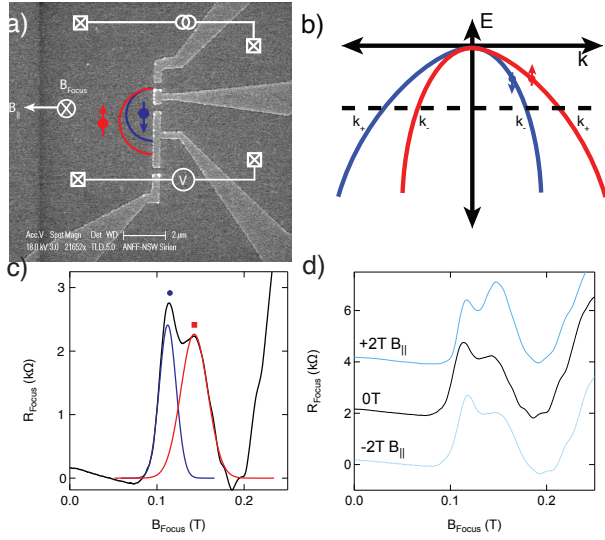


FIG. 1. Spin-resolved focussing with in-plane magnetic fields **a)** SEM of the focussing sample. The overlay shows the orientation of the in-plane (B_{\parallel}) and out-of-plane (B_{Focus}) magnetic fields, as well as the electrical setup for measurements. Red and blue semicircles indicate the spin-split focussing trajectories. **b)** The first 2D subband for holes. A Rashba spin-orbit interaction causes a spin-splitting of the subband resulting in two different momenta (k_+ and k_-) at the Fermi energy (horizontal dashed line). This difference in momentum results in different focussing trajectories for each spin. **c)** The spin split first focussing peak resulting from the two spin-dependent focussing trajectories (labelled with blue circle and red square). By fitting a double Gaussian to the first focussing peak the amplitude of both peaks can be extracted. **d)** Spin split focussing with an in-plane magnetic field. The change in peak amplitude is not symmetric when the direction of the in-plane field is reversed.

at base temperature (30mK). In-plane and out-of-plane fields are also measured using Hall sensors on the sample probe to correct for any magnet hysteresis.

In GaAs hole systems, spin-orbit interactions have a significant effect on magnetic focussing measurements. The Rashba spin-orbit interaction causes a spin splitting of the first 2D subband which results in a different momentum for each spin. Figure 1 b) shows the spin-split first 2D subband for holes in GaAs, with the red and blue bands representing the different spins. The splitting of the 2D subband results in a difference of momentum between the spins (k_+ and k_-) at the Fermi energy (horizontal dashed line). The different momentum creates a different focussing trajectory for each spin, which splits the first focussing peak [27]. The splitting of the 2D subband can also create a different scattering rate for each spin, as it changes the slope of each subband and hence the velocity. The relatively symmetric quantum well heterostructure used in this work allows for visible spin splitting while also giving a similar scattering rate for both spin states [26].

Figure 1 c) shows focussing with no in-plane magnetic field. A double peak is observed consistent with spin-resolved focussing, with additional small oscillations due to the Shubnikov-de Haas effect and path interference [16, 24]. Above $B_{Focus} = 0.2T$ the resistance increases due to the onset of the second classical focussing peak. A double Gaussian fit to the split peak (red and blue peaks in Fig. 1 c) shows that both peaks have a similar amplitude in the absence of an in-plane magnetic field. The higher field (red square) peak is also broader due to the previously mentioned path interference and a difference in scattering [24, 26]. Figure 1 d) shows the first focussing peak with a magnetic field applied in-plane parallel to the QPC current direction (B_{\parallel}). With $B_{\parallel} = +2T$ (top trace - blue), a clear change in the peak amplitude is observed compared to the peaks with no in-plane field (black centre trace). This change in peak amplitude would typically be interpreted as a change in the spin polarisation [27]. However, when the direction of B_{\parallel} is reversed to $-2T$ (bottom trace in Fig. 1 d) the change in peak amplitude is not symmetric. This is not consistent with a change in spin polarisation as the Zeeman splitting should be the same for $\pm B_{\parallel}$.

To rule out any Zeeman or spin polarisation effects, we next measure the change in peak amplitude with small in-plane magnetic fields. Figure 2 a) shows the results of focussing with small B_{\parallel} applied in 0.1T increments up to $\pm 0.5T$. A double Gaussian is fitted to each peak and the amplitude as a function of B_{\parallel} is plotted in Fig. 2 b). A change in amplitude of the spin peaks is observed for fields as small as $\pm 0.1T$, far too small to be caused by a change in spin polarisation. Even at 0.5T the change in peak amplitude ($\sim 10\%$) is significantly larger than the Zeeman energy ($\sim 1\%$ of E_F) and therefore is too small to be a Zeeman effect. Instead, we consider a shift in the Rashba spin-splitting of the 2D subbands caused by B_{\parallel} .

The Hamiltonian for the 2D subbands is of the form

$$\mathcal{H} = \frac{\mathbf{p}^2}{2m^*} + \frac{i\alpha}{2}(\sigma_+ p_-^3 - \sigma_- p_+^3) + \frac{g_1 \mu_B}{2}(B_+ p_+^2 \sigma_- + B_- p_-^2 \sigma_+) + \frac{g_2 \mu_B}{2}(B_- p_+^4 \sigma_- + B_+ p_-^4 \sigma_+) \quad (1)$$

where $\frac{i\alpha}{2}(\sigma_+ p_-^3 - \sigma_- p_+^3)$ is the Rashba spin-orbit term, $\frac{g_1 \mu_B}{2}(B_+ p_+^2 \sigma_- + B_- p_-^2 \sigma_+) + \frac{g_2 \mu_B}{2}(B_- p_+^4 \sigma_- + B_+ p_-^4 \sigma_+)$ are the Zeeman terms due to the in-plane magnetic field and $B_{\pm} = B_x \pm iB_y$. B_{\parallel} causes a small shift in the 2D spin subbands, which is in opposite directions for the two subbands. Figure 2 c) shows the calculated energy dispersion of one of the 2D hole subbands using Eq. 1. There is a small shift in the subband dispersion, which is not the same for $\pm B_{\parallel}$. This shift is too small to cause a measurable change in the location of the magnetic focussing peaks, however it will still cause a change in the subband curvature [24, 31, 32]. The change in subband curvature causes the Fermi velocity (v_F) to change along the hole trajectory. v_F is linked to the scattering rate of

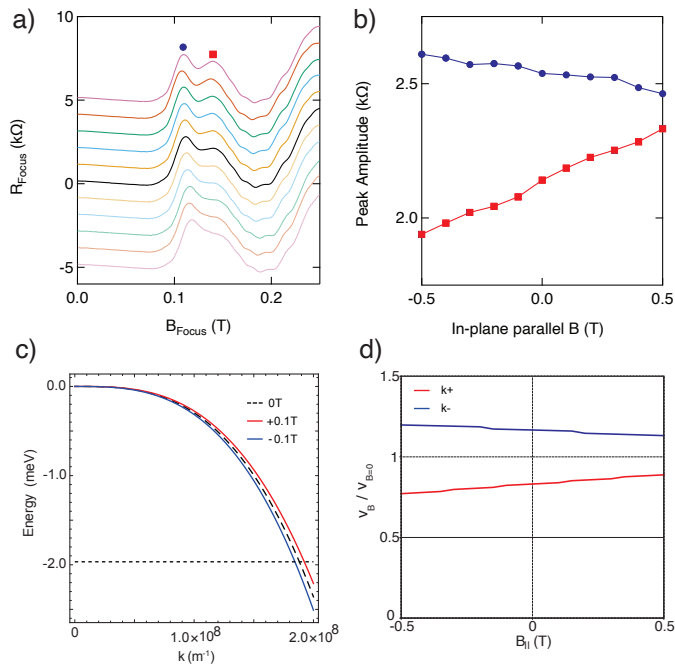


FIG. 2. **Focussing with small B in-plane parallel to the QPC orientation.** **a)** Shows the focussing signal for different in-plane fields of ± 0.5 T in 0.1 T steps. Central black trace is for zero field, top solid traces are for field parallel to the QPC current and bottom dashed traces are for field antiparallel. Data has been vertically offset for clarity. **b)** The amplitude of each spin peak from a double Gaussian fit to the data in a). **c)** The calculated energy dispersion of one of the spin-split 2D hole subbands for $B_{\parallel} = +0.1$ T, 0T and -0.1 T using Eq 1. The dashed horizontal line is the Fermi energy. **d)** The change in velocity of the spin subbands as a function of B_{\parallel} . The calculated velocity of each spin state (v_B) is normalised by the average velocity of the two spins at $B_{\parallel} = 0$ ($v_{B=0}$).

each spin, since holes that travel slower will have more time to scatter (and vice versa). The focussing peak amplitude is exponentially sensitive to v_F :

$$R_{Focuss} \propto e^{-\pi d / (2v_F \tau_{Focuss})} \quad (2)$$

where d is the focussing diameter and $v_F \tau_{Focuss}$ is the characteristic focussing scattering length [17, 26, 33]. Figure 2 d) shows the calculated change in v_F for small B_{\parallel} . This matches the trend in focussing peak amplitude shown in Fig. 2 b) (see supplementary info for further comparison). This change in focussing peak amplitude for small B_{\parallel} demonstrates the high sensitivity of focussing to small changes in the Fermi surface.

Next, we consider shifts in the Fermi surface caused by large B_{\parallel} . Figure 3 a) shows the evolution of the first focussing peak with a large in-plane magnetic field applied parallel to the QPC current direction (B_{\parallel}). As B_{\parallel} increases in magnitude the peak amplitude changes, which would typically interpreted as a change in spin polarisation. Again, when the polarity of B_{\parallel} is reversed (Fig. 3

b), the change in peak amplitude is not symmetric. This is not consistent with a change in spin polarisation as Zeeman splitting should be the same for $\pm B_{\parallel}$. To make this clearer, the amplitude of the spin peaks is plotted as a function of B_{\parallel} in Fig. 3 c). The peak amplitude is clearly not symmetric around $B_{\parallel} = 0$. This amplitude change is consistent across multiple measurements and fitting procedures (e.g. fitting the peak area). See supplementary info for further details. If the change in peak amplitude was due to Zeeman spin polarisation there should be a monotonic response in the amplitude. This is not visible in Fig. 3 c), providing further evidence that the change in peak amplitude is not a Zeeman effect or a change in spin polarisation. Furthermore, this amplitude change is not a result of a distortion of the Fermi surface due to B_{\parallel} , as this distortion should also be symmetric for $\pm B_{\parallel}$. In addition, the asymmetry in the amplitude change is not an artefact of the setup, as it meets the Onsager reciprocity conditions ($\pm B_{\parallel}$ symmetry is restored if the field direction is reversed and the current and voltage probes are swapped - see supplementary info).

The non-monotonic change in the focussing peak amplitude can be explained by a shift in the spin-split Fermi surfaces caused by B_{\parallel} . Figure 4 shows the calculated shift in the spin-split Fermi surfaces using Eq. 1. Figure 4 a) shows the section of the Fermi surface measured by focussing in the absence of B_{\parallel} . The red and blue lines indicate the calculated spin-split Fermi surface. The solid section corresponds to the focussing trajectory, while the dashed side does not contribute to focussing. At $B_{\parallel} = 0$ T the spacing between the blue and red subbands is the same for all points on the Fermi surface. Figure 4 b) shows the change in Fermi surface for $B_{\parallel} = +4$ T. The in-plane field causes the blue Fermi surface to shift towards $k=0$, while the red surface is shifted away. Since only the solid parts of the Fermi surfaces contribute to focussing, these paths move further apart, leading to more adiabatic transport. When the direction of B_{\parallel} is reversed (Fig. 4 c), the blue Fermi surface shifts away from $k=0$, while the red surface shifts towards $k=0$. The solid sections of the Fermi surfaces now almost touch, allowing mixing between the spin states. This results in non-adiabatic spin evolution [34] and causes a significant shift in the amplitude and position of the focussing peaks at $B_{\parallel} = -4$ T as shown in Fig. 3 b). This asymmetry in the Fermi surface shift is not observed in other 2D measurements (e.g. Shubnikov-de Haas oscillations) since they sample the full Fermi surface and hence would see the same result for $+B_{\parallel}$ and $-B_{\parallel}$.

In summary, we have used magnetic focussing to measure a change in parity of spin-split Fermi surfaces caused by B_{\parallel} . For small B_{\parallel} the centre of the Fermi surface shifts, resulting in a change in velocity and hence scattering along the two spin resolved focussing trajectories. At large B_{\parallel} , the spin-split Fermi surfaces touch, leading to non-adiabatic transport for one particular direction of

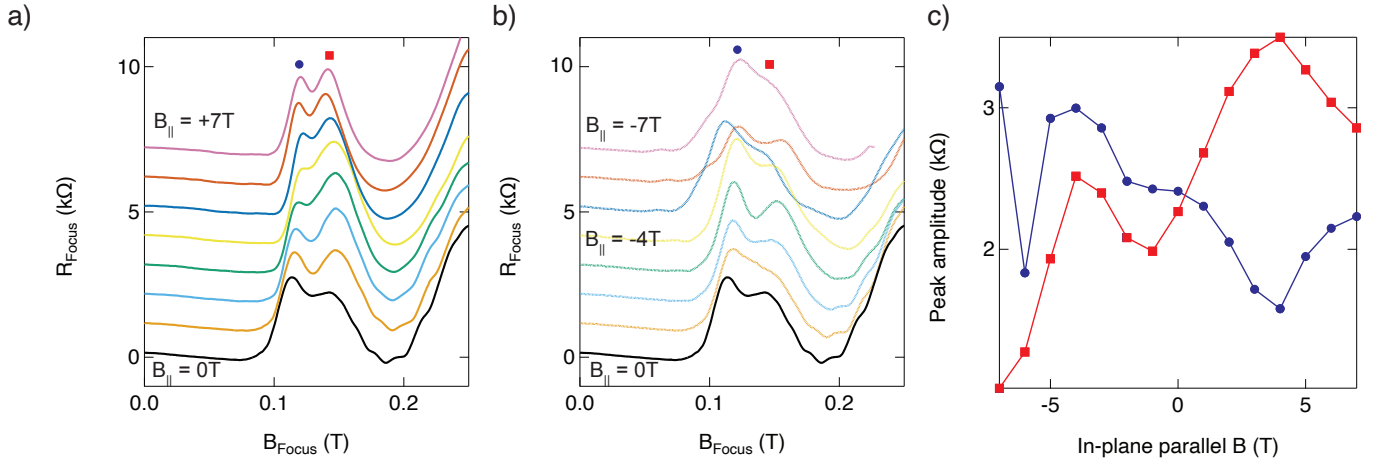


FIG. 3. **Focussing with a large B in-plane parallel to the QPC current.** **a)** The focussing signal with an in-plane field applied along the QPC up to $+7$ T in 1 T steps. The black trace is for zero in-plane field. Each trace has been vertically offset by 1 k Ω for clarity. **b)** The same as in **a)** with the opposite polarity of in-plane magnetic field. **c)** The amplitude of each spin peak as from a fit to each focussing trace. Error bars from the peak fit are smaller than the markers.

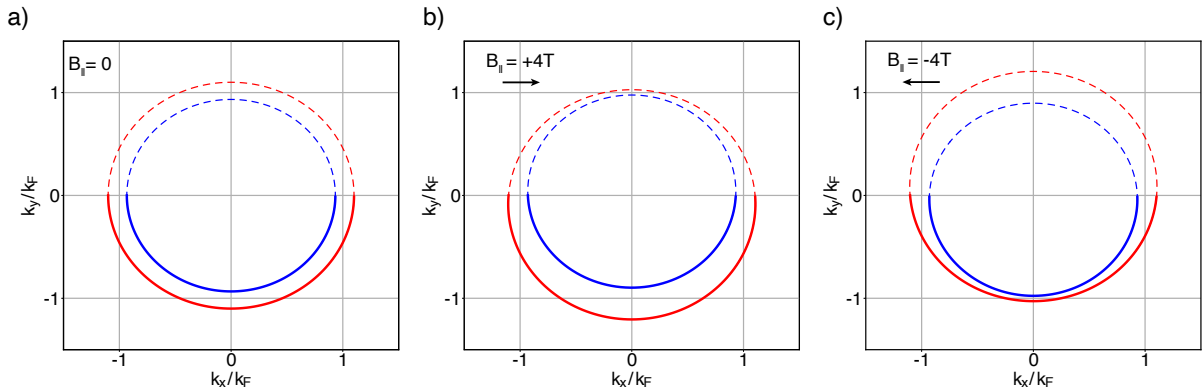


FIG. 4. **Calculated spin split Fermi surface shift with $B_{\parallel} = \pm 4$ T** **a)** With no B_{\parallel} . Red and blue circles correspond to the 2D spin sub-bands. Solid lines indicates the section of the Fermi surfaces over which focussing measurements are performed. **b)** With $B_{\parallel} = +4$ T, separation of the two spin-split Fermi surfaces is increased over focussing trajectories. **c)** With $B_{\parallel} = -4$ T, Fermi surfaces almost touch leading to non-adiabatic spin dynamics.

the applied B_{\parallel} . This non adiabatic transport causes a significant shift in the focussing peaks. Neither of these effects can be explained by a change in spin polarisation or a Zeeman effect. These results show that magnetic focussing can be used to detect changes in parity of the 2D Fermi surface, as well as its extreme sensitivity to Fermi surface changes. In addition, these effects can only be measured via magnetic focussing as it is able to probe a section of the Fermi surface, unlike other 2D measurements such as Shubnikov-de Haas or commensurability oscillations. While this work has focussed on a change in parity due to the spin-orbit interaction of holes in GaAs, this technique should be applicable to similar changes in the Fermi surface of other 2D systems.

The authors would like to thank U. Zülicke and Z. Krix for many valuable discussions. Devices

were fabricated at the UNSW node of the Australian National Fabrication Facility (ANFF). This research was funded by the Australian Government through the Australian Research Council Discovery Project Scheme; Australian Research Council Centre of Excellence FLEET (project number CE170100039); and by the the UK Engineering and Physical Sciences Research Council (Grant No. EP/R029075/1). All experimental data and calculation code is available at <http://dx.doi.org/10.5281/zenodo.8368876>

* M. J. Rendell and S. D. Liles contributed equally to this work

[1] W. J. de Haas and van Alphen, Proceeding of the Nether-

- lands Royal Academy of Sciences **33**, 1106 (1930).
- [2] L. Schubnikow and W.J. de Haas, *Nature* **126**, 500 (1930).
- [3] G. Lonzarich, *Journal of Magnetism and Magnetic Materials* **76-77**, 1 (1988).
- [4] N. E. Hussey, M. Abdel-Jawad, A. Carrington, A. P. Mackenzie, and L. Balicas, *Nature* **425**, 814 (2003).
- [5] N. Doiron-Leyraud, C. Proust, D. LeBoeuf, J. Levallois, J.-B. Bonnemaïson, R. Liang, D. A. Bonn, W. N. Hardy, and L. Taillefer, *Nature* **447**, 565 (2007).
- [6] S. Danzenbächer, D. V. Vyalikh, K. Kummer, C. Krellner, M. Holder, M. Höppner, Y. Kucherenko, C. Geibel, M. Shi, L. Patthey, S. L. Molodtsov, and C. Laubschat, *Physical Review Letters* **107**, 267601 (2011).
- [7] D. E. Soule, J. W. McClure, and L. B. Smith, *Physical Review* **134**, A453 (1964).
- [8] S. Askenazy, J.-P. Ulmet, J. Léotin, L. Holan, and A. Laurent, *Solid State Communications* **7**, 717 (1969).
- [9] R. W. Shaw and D. E. Hill, *Physical Review B* **1**, 658 (1970).
- [10] B. Brosh, M. Y. Simmons, S. N. Holmes, A. R. Hamilton, D. A. Ritchie, and M. Pepper, *Physical Review B* **54**, R14273 (1996).
- [11] E. Skuras, A. Long, I. Larkin, J. Davies, and M. Holland, *Applied Physics Letters* **70**, 871 (1997).
- [12] D. Kamburov, M. Shayegan, R. Winkler, L. Pfeiffer, K. West, and K. Baldwin, *Physical Review B* **86**, 241302 (2012).
- [13] Y. Sharvin, *Soviet Journal of Experimental and Theoretical Physics* **48**, 984 (1965).
- [14] V. Tsoi, *Soviet Journal of Experimental and Theoretical Physics* **19**, 114 (1974).
- [15] V. Tsoi, *Physica B: Condensed Matter* **48**, 14679 (1996).
- [16] H. van Houten, C. W. J. Beenakker, J. G. Williamson, M. E. I. Broekaart, P. H. M. van Loosdrecht, B. J. van Wees, J. E. Mooij, C. T. Foxon, and J. J. Harris, *Physical Review B* **39**, 8556 (1989).
- [17] J. Heremans, M. Santos, and M. Shayegan, *Applied Physics Letters* **61**, 1652 (1992).
- [18] J. Heremans, M. Santos, and M. Shayegan, *Surface science* **305**, 348 (1994).
- [19] T. Taychatanapat, K. Watanabe, T. Taniguchi, and P. Jarillo-Herrero, *Nature Physics* **9**, 225 (2013).
- [20] M. Lee, J. R. Wallbank, P. Gallagher, K. Watanabe, T. Taniguchi, V. I. Fal'ko, and D. Goldhaber-Gordon, *Science* **353**, 1526 (2016).
- [21] M. D. Bachmann, A. L. Sharpe, A. W. Barnard, C. Putzke, M. König, S. Khim, D. Goldhaber-Gordon, A. P. Mackenzie, and P. J. W. Moll, *Nature Communications* **10**, 5081 (2019).
- [22] A. I. Berdyugin, B. Tsim, P. Kumaravadivel, S. G. Xu, A. Ceferino, A. Knothe, R. K. Kumar, T. Taniguchi, K. Watanabe, A. K. Geim, I. V. Grigorieva, and V. I. Fal'ko, *Science Advances* **6**, eaay7838 (2020).
- [23] K. Aidala, R. Parrott, T. Kramer, E. Heller, R. Westervelt, M. Hanson, and A. Gossard, *Nature Physics* **3**, 464 (2007).
- [24] S. Bladwell and O. P. Sushkov, *Physical Review B* **98**, 085438 (2018).
- [25] A. Gupta, J. J. Heremans, G. Kataria, M. Chandra, S. Fallahi, G. C. Gardner, and M. J. Manfra, *Nature Communications* **12**, 5048 (2021).
- [26] M. J. Rendell, S. D. Liles, A. Srinivasan, O. Klochan, I. Farrer, D. A. Ritchie, and A. R. Hamilton, *Physical Review B* **107**, 045304 (2023).
- [27] L. P. Rokhinson, V. Larkina, Y. B. Lyanda-Geller, L. N. Pfeiffer, and K. W. West, *Physical Review Letters* **93**, 146601 (2004).
- [28] S.-T. Lo, C.-H. Chen, J.-C. Fan, L. W. Smith, G. L. Creeth, C.-W. Chang, M. Pepper, J. P. Griffiths, I. Farrer, H. E. Beere, G. A. C. Jones, D. A. Ritchie, and T.-M. Chen, *Nature Communications* **8**, 15997 (2017).
- [29] A. M. See, I. Pilgrim, B. C. Scannell, R. D. Montgomery, O. Klochan, A. M. Burke, M. Aagesen, P. E. Lindelof, I. Farrer, D. A. Ritchie, R. P. Taylor, A. R. Hamilton, and A. P. Micolich, *Physical Review Letters* **108**, 196807 (2012).
- [30] A. Srinivasan, I. Farrer, D. A. Ritchie, and A. R. Hamilton, *Applied Physics Letters* **117**, 183101 (2020).
- [31] S. Bladwell and O. P. Sushkov, *Physical Review B* **92**, 235416 (2015).
- [32] E. Marcellina, A. Srinivasan, D. S. Miserev, A. F. Croxall, D. A. Ritchie, I. Farrer, O. P. Sushkov, D. Culcer, and A. R. Hamilton, *Physical Review Letters* **121**, 077701 (2018).
- [33] M. Rendell, O. Klochan, A. Srinivasan, I. Farrer, D. Ritchie, and A. Hamilton, *Semiconductor Science and Technology* **30**, 102001 (2015).
- [34] C. Zener, *Proceedings of the Royal Society A* **137**, 696 (1932).